Geomechanics and Engineering, *Vol. 12, No. 4 (2017) 657-673*
DOI: https://doi.org/10.12989/gae.2017.12.4.657

In situ investigations into mining-induced overburden failures in close multiple-seam longwall mining: A case study

Jianguo Ning [1a], Jun Wang [*1], Yunliang Tan [**1],
Lisheng Zhang [2b] and Tengteng Bu [1c]

[1] *A State Key Laboratory of Mining Disaster Prevention and Control Co-founded by Shandong Province and the Ministry of Science and Technology, Shandong University of Science and Technology, 579 Qianwangang Road, Qingdao, China*
[2] *Gaojiangliang Colliery, Haohua Cleaned Coal Co., Ltd, Erdos City, Inner Mongolia, China*

(*Received September 14, 2016, Revised December 08, 2016, Accepted December 26, 2016*)

Abstract. Preventing water seepage and inrush into mines where close multiple-seam longwall mining is practiced is a challenging issue in the coal-rich Ordos region, China. To better protect surface (or ground) water and safely extract coal from seams beneath an aquifer, it is necessary to determine the height of the mining-induced fractured zone in the overburden strata. In situ investigations were carried out in panels 20107 (seam No. $2\text{-}2^{\text{upper}}$) and 20307 (seam No. $2\text{-}2^{\text{middle}}$) in the Gaojialiang colliery, Shendong Coalfield, China. Longwall mining-induced strata movement and overburden failure were monitored in boreholes using digital panoramic imaging and a deep hole multi-position extensometer. Our results indicate that after mining of the 20107 working face, the overburden of the failure zone can be divided into seven rock groups. The first group lies above the immediate roof (12.9 m above the top of the coal seam), and falls into the gob after the mining. The strata of the second group to the fifth group form the fractured zone (12.9-102.04 m above the coal seam) and the continuous deformation zone extends from the fifth group to the ground surface. After mining Panel 20307, a gap forms between the fifth rock group and the continuous deformation zone, widening rapidly. Then, the lower portion of the continuous deformation zone cracks and collapses into the fractured zone, extending the height of the failure zone to 87.1 m. Based on field data, a statistical formula for predicting the maximum height of overburden failure induced by close multiple seam mining is presented.

Keywords: close multiple-seam mining; overburden structure; failure zone; in situ investigations

1. Introduction

The Ordos region is located in a semi-arid desert region in northwest China, where the ecological system is fragile. Ordos coal reserves account for one-third of the total coal reserves of China; thus, this region is expected to provide a substantial part of China’s energy resources in the

*Corresponding author, Ph.D., E-mail: wangjunsdkjd@126.com
**Corresponding author, Professor, E-mail: tylllp@163169.net
[a] Professor, E-mail: njglxh@126.com
[b] Senior Engineer, E-mail: 275247369@qq.com
[c] Student, E-mail: 460372633@qq.com

http://www.techno-press.org/?journal=gae&subpage=7 ISSN: 2005-307X (Print), 2092-6219 (Online)

next century (Miao *et al*. 2011, Zhang *et al*. 2011). It is not uncommon to find up to 10 coal seams within a 100-250 m thick layer, more than half of which are mineable. As shown in Fig. 1, the mineable coal seams are of the Jurassic period and are typically overlain by a very thick layer of soft rock with poor cementation (Jin and Zhang 2010). Multiple-seam mining is common in the Ordos region (Zhang *et al*. 2014, Wang *et al*. 2015). As shown in Fig. 2, large-scale close multiple-seam longwall mining can disturb or even damage the overburden strata, with the most severe damage occurring near the immediate roof and decreasing toward the ground surface. Such damage can lead to considerable groundwater seepage or even inrush into the mine and disturb the vulnerable ecological environment. Protection of the water resources affected by the large-scale and highly-efficient mining of close multiple seams in the Ordos region is an ongoing challenge for the coal mining industry in the region (Zhang *et al*. 2011, Ma *et al*. 2013). To reduce the risk of water-induced damage and accidents and to protect the surface (or ground) water, we need to improve our understanding of strata movement and overburden failure induced by large-scale close longwall mining.

Extensive studies on mining-induced overburden movement and failure were conducted, with broad understanding and practical knowledge gained (Palchik 2010, Rezaei *et al*. 2015, Khanal *et*

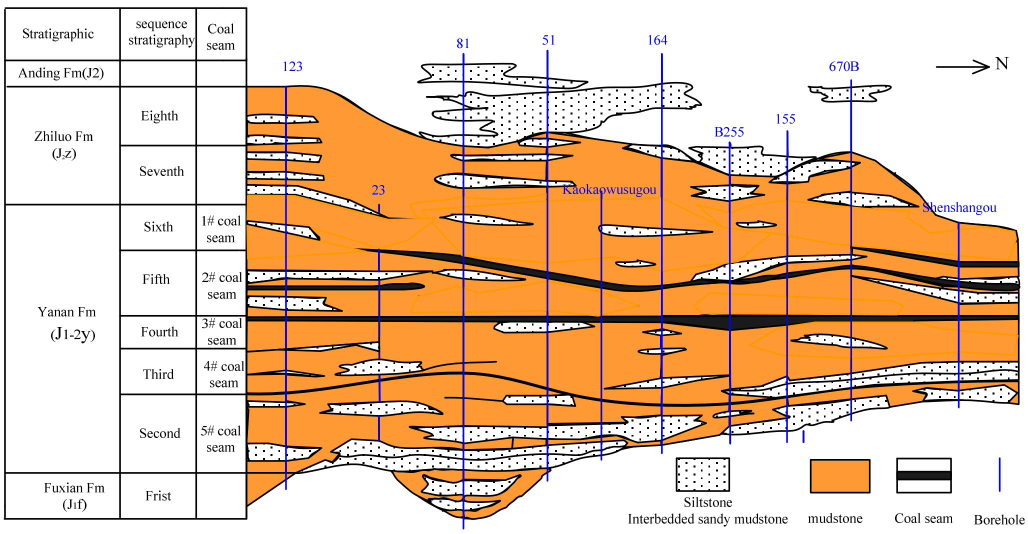

Fig. 1 Simplified stratigraphic section in the Ordos coalfield (Jin *et al*. 2010)

Fig. 2 Surface cracks in Quaternary soils of the Gaojialiang coal mine

al. 2016, Wang *et al*. 2016, Tan *et al*. 2017). Earlier research found that the movement of overburden rock strata in response to longwall mining can be divided into three zones, from the upper surface of the coal seam to the ground surface: the caved zone, the fractured zone, and the continuous deformation zone (Xiong *et al*. 2015, Tulu *et al*. 2016). Physical modeling, numerical analyses, and in situ investigations were used to measure the caved and fractured zones (Palchik 2010, Miao *et al*. 2011, Zhang *et al*. 2011, Gao *et al*. 2014, Sui *et al*. 2015). Some relevant studies showed that the combined thickness of the caved and fractured zones depends strongly on the strata lithology, mining geometry, and mining methods (Palchik 2010, Rezaei *et al*. 2015, Khanal *et al*. 2016, Wang *et al*. 2016). In China, the movement of overburden induced by coal seam mining was extensively studied, particularly cases where the overburden roof strata consisted of hard and strong or medium-strong rock (Miao *et al*. 2011, Guo *et al*. 2012, Karacan and Olea 2015). These investigations showed that the combined thickness of the caved and fractured zones was between 20 and 60 times the mining height. In the 1980s, based on field data from China, the National Coal Ministry Administration of China set national standards for mining of coal seams (Yu *et al* 2015), these standards affect the safety of buildings, water bodies, railways, etc. The standards include experimental data of caved and fractured zones and statistical formulas of the combined heights of these two zones that apply to coal seam mining where the overlying rock is hard and strong, or medium-strong.

Many studies were recently carried out using various methods to investigate the movement of overburden strata induced by the mining of a single coal seam (Miao *et al*. 2011, Zhang *et al*. 2011, Ma *et al*. 2013, Liu *et al*. 2015, Zhao 2015). These studies showed that in situ measurements of the failure zone were very limited in the Ordos region, where coal seams are typically overlain by a very thick soft rock layer (mudstone or sandy mudstone) with poor cementation, in particular, when close multiple-seam longwall mining was practiced. However, our understanding of overburden failure caused by close multiple-seam mining is limited compared with our knowledge regarding single-seam mining. Specifically, the mechanism of overburden failure induced by close multiple-seam longwall mining needs further investigation, as well as the commonly used statistical formulas for predicting the height of the failure zone.

In this study, we performed in-situ investigations of the failure zone of overburden strata induced by close multiple-seam mining in the Ordos region. First, the fracturing process of the overburden strata, caused by close multiple-seam mining, was examined. Second, the structure of the overburden failure was determined. Finally, a model to describe the failure zone of the overburden was developed. Moreover, a detailed description of the experimental equipment used in the investigation is presented, as well as an analysis of the field data and a statistical formula for predicting the maximum height of the overburden failure induced by close multiple-seam mining.

2. Geological background, mine layout, and experimental design

2.1 Geological and mining conditions of the longwall face

The Gaojialiang mine is located in Ordos City, Inner Mongolia Autonomous region, China. The mining area lies in a region of urban development; however, the semi-arid climate presents many environmental challenges such as dry climate, poor soil, and sparse vegetation. There are six key mineable coal seams in the Gaojialiang mine, which are of the Jurassic period. Those coal seams are numbered No. $2\text{-}2^{\text{upper}}$, No. $2\text{-}2^{\text{middle}}$, No. 3-1, No. $4\text{-}2^{\text{middle}}$, No. 5-1, and No. $6\text{-}2^{\text{middle}}$, among which coal seams No. $2\text{-}2^{\text{upper}}$ and No. $2\text{-}2^{\text{middle}}$ are currently being mined. Both the upper seam, No.

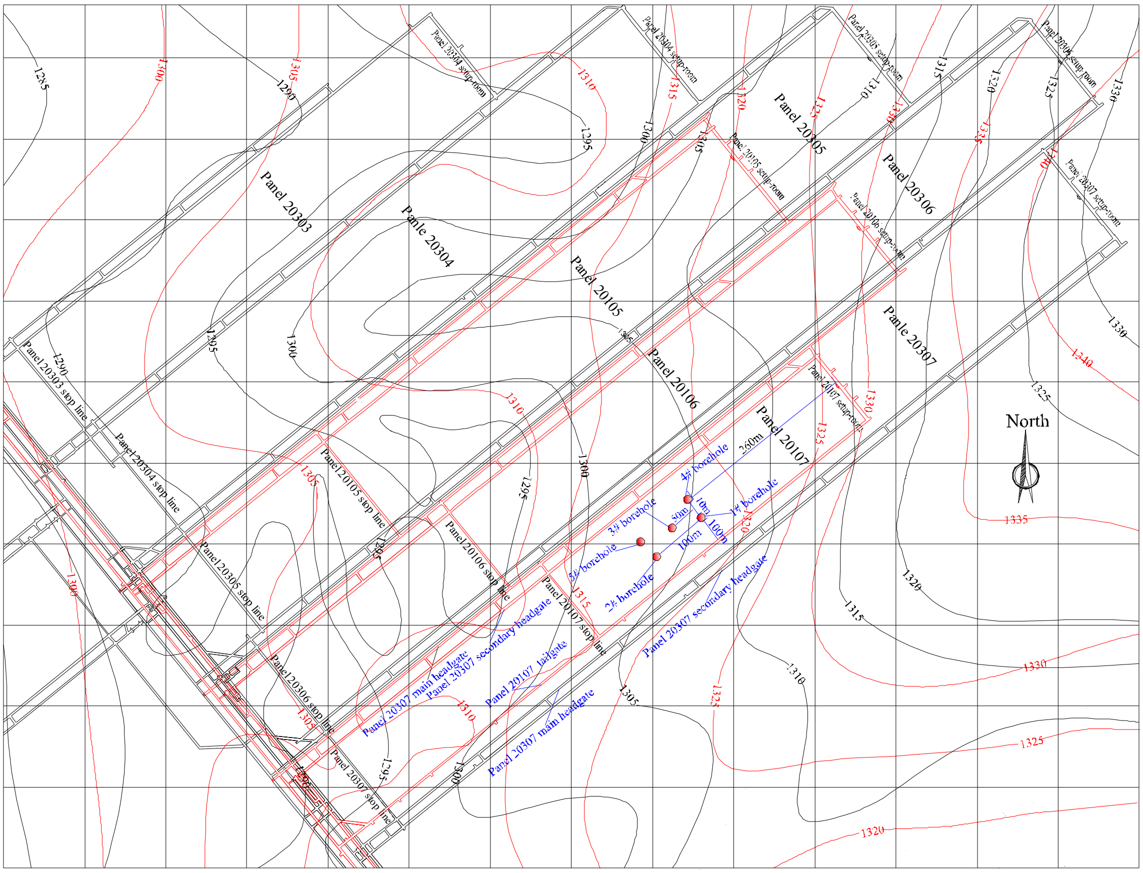

Fig. 3 Plan view of local panel layout

2-2^{upper}, and the lower seam, No. 2-2^{middle}, are nearly horizontal with a mean thickness of 4.10 m and 5.2 m, respectively, and interburden thicknesses of 9.5 m. The buried depth of the two seams is 253 m and 262.5 m, respectively. Close multiple-seam longwall mining is practiced in this mine and the retreating longwall method is used in all of the panels. Panels 20105, 20106, and 20107 are worked in seam No. 2-2^{upper} and panels 20303–20307 are worked in seam No. 2-2^{middle} (Fig. 3). Currently, Panels 20105, 20106, 20303, 20304, 20305, and 20306 have been extracted. In this study we focus on Panels 20107 and 20307. Panels 20107 and 20307 are approximately 200 m and 260 m along the dip, and 1650 m and 1560 m along the strike, respectively. They were mined by the retreat LW mining method with full seam extraction at an average rate of 8 m per day. A simplified stratigraphic column of Panel 20107 based on drilled cores is shown in Fig. 4. The roof strata of this panel are composed mainly of sandy mudstone, mudstone, and siltstone, with a uniaxial compressive strength less than 20 MPa. These overburden rocks are classified as soft and weak.

2.2 Experimental method

2.2.1 Deephole multi-position extensometer

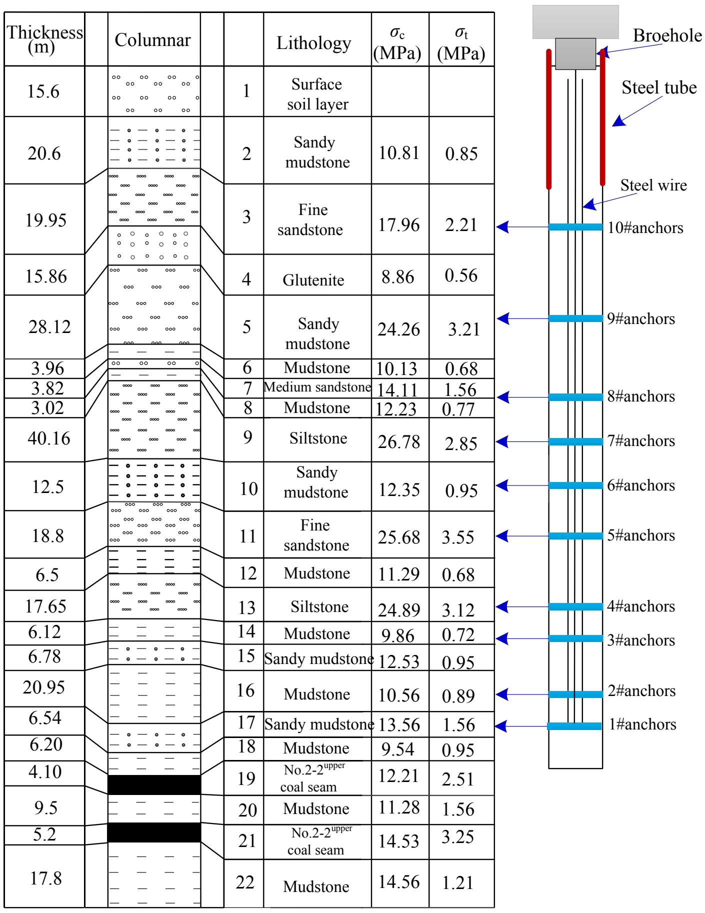

Note: σ_t is tensile strength, σ_c is uniaxial compressive strength

Fig. 4 Typical geological column of Panel 20107 based on drill cores

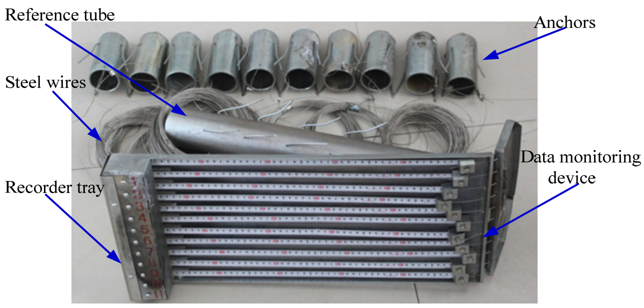

Fig. 5 Deephole multi-position extensometer for accurate displacement measurements

To identify the longwall mining-induced strata movement, a deephole multi-position extensometer (DMPX) (UROICAC. Ltd., China), was used (Fig. 5). It consists of high tensile stainless steel wires, anchors, a reference tube, recorder tray, and data monitoring device. The end of each

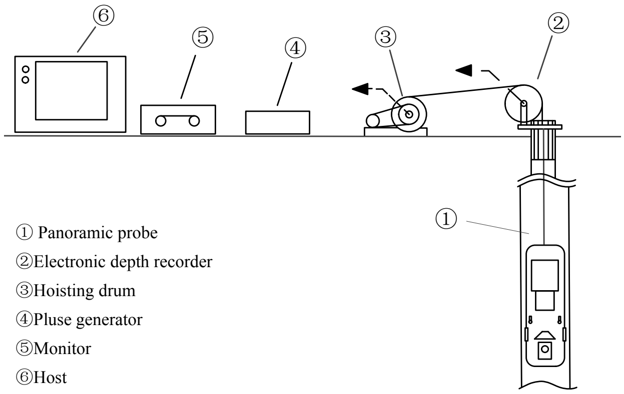

Fig. 6 Illustration of DPID

high-tensile stainless steel wire is connected to an anchor and up to 10 anchors can be placed in one borehole. The other end of the wire is connected to the data monitoring device, which measures the change in the length of the wire that extends out from the recorder tray. This provides a physical method of measuring the displacement in the overburden strata between the working panel and the surface. The measurement accuracy of the DMPX is ±1 mm, which meets practical engineering requirements.

2.2.2 Digital panoramic imaging device

To determine the longwall mining-induced strata failure, a digital panoramic imaging device (DPID) (UROICAC Ltd., China) was used (Fig. 6). It consists of the following basic components:

(1) A panoramic probe containing a digital CCD video camera, 25 mm in diameter and 100 mm in length. It scans the macro-fractures of the borehole wall without external disturbance.
(2) A cable data line, 5 mm in diameter, which can efficiently and clearly transmit videos or images from the probe to the host. The probe is lowered to the required depth in the borehole at a speed of about 20 mm/s by a hoisting drum located on the ground surface.
(3) An electronic depth recorder that records the depth of the probe in the borehole by measuring the change in the length of the data line extended from the host.
(4) The host – a microcomputer that receives, stores (up to 8 Gb), and displays the videos or images from the probe and supplies power (from a 3V lithium battery) to the probe.

The measurement accuracy of the DPID is ±1 mm and the effective detecting depth is 0-300 m. The host is supported by high-capacity lithium batteries which can power the DPID in work mode continuously for more than 24 hours. These specifications satisfy the requirements of most engineering applications.

3. Experimental procedure

For the field measurements, five vertical boreholes were drilled (Figs. 3 and 7). Before the mining of Panel 20107, boreholes #1, #2, and #3 were drilled from the ground surface to the extracted coal seam. Before Panel 20307 was mined, boreholes #4 and #5 were also drilled.

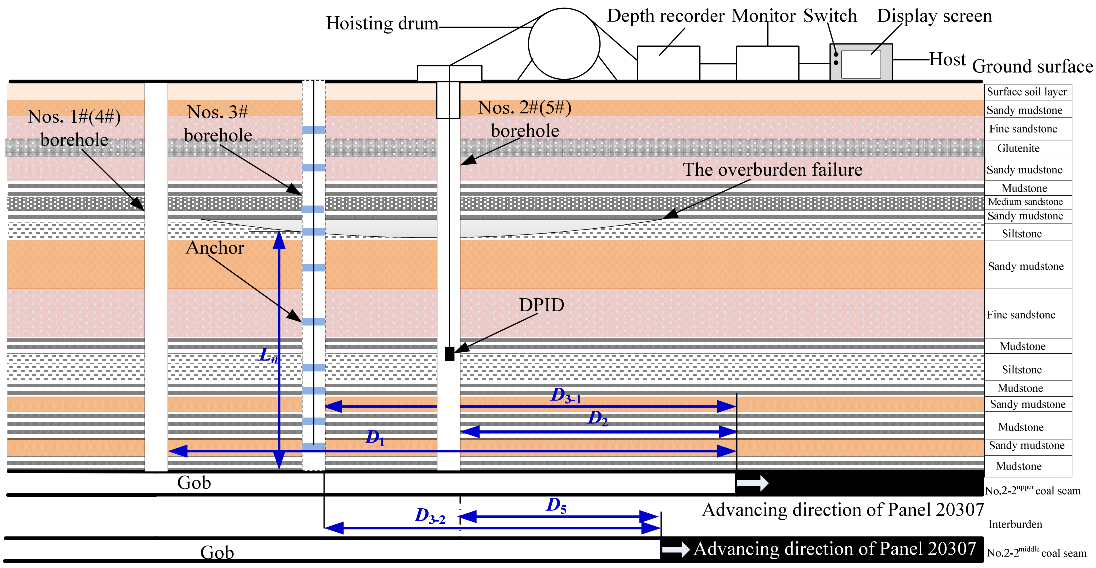

Fig. 7 Illustration of layout for field investigation

Boreholes #1, #2, #4, and #5 were all 253 m long and 105 mm in diameter; the data from these boreholes was recorded by the DPID and used to analyze the overburden failures. Boreholes #1 and #2 were located in the middle of Panel 20107 and set 100 m apart horizontally and 260 m and 360 m from the set-up room of Panel 20107, respectively, 100 m from the air-return roadway. Boreholes #4 and #5 were located in the middle of Panel 20307, 100 m apart horizontally and both located 560 m from the set-up room of Panel 20107. Borehole #3 was 50 mm in diameter and 253 m in length; the data recoded in borehole #3 was transmitted to the DMPX and used to study the overburden movement.

The experimental setup used for measuring the movement of the strata above the longwall panel is shown in Fig. 7. The horizontal distances from Panel 20107 to boreholes #1, #2, and #3 were denoted D_1, D_2, and $D_{3\text{-}1}$, respectively. $D_{3\text{-}2}$, D_4, and D_5 were defined as the horizontal distances from Panel 20307 to boreholes #3, #4, and #5, respectively. The distance ahead of the longwall face (before the face passes the location of the borehole) is denoted as negative D_m (m = 1, 2, 3-1, 3-2, 4, and 5) while for distances behind the longwall face (after it has passed beneath the borehole) D_m is taken as positive. To investigate the overburden strata behavior, the following experimental step was conducted.

Step 1: before Panel 20107 of coal seam No. 2-2$^{\text{upper}}$ was mined, boreholes #1, #2, and #3 were drilled as shown in Fig. 3. To record the original state of the borehole walls (before mining commenced), the borehole walls were scanned by the DPID camera and the videos were transmitted from the host to the processing computer. Then the DMPX was applied at borehole #3 and 10 anchors were installed to monitor the overburden movement. The locations of the anchors are shown in Fig. 4. The strata displacement was observed by DMPX every day until the extraction of Panel 20107 of coal seam No. 2-2$^{\text{upper}}$ was completed.

Step 2: before the mining of Panel 20307 of coal seam No. 2-2$^{\text{middle}}$, boreholes #4 and #5 were drilled according to the plan.

Step 3: for 0 m $\leq D_{m\ (m\,=\,1,\,2,\,4,\,5)} \leq$ 30 m, the probe was lowered into the borehole and the borehole wall was scanned daily by the DPID from the top of the coal seam or the top surface of the caved rock layers 30 m upwards. Scanned videos of the macro-fracture development and failure extent at the borehole wall were obtained, and transmitted from the host to the processing computer.

Step 4: for 30 m $\leq D_{m\ (m=1,2,4,5)} \leq$ 100 m, the borehole wall was scanned from the top of the coal seam or the top surface of the caved zones 30 m upwards. The measurements were conducted after the longwall face advanced 10 m. Then, the actions outlined in step 3 were repeated.

Step 4: for 100 m $\leq D_{m\ (m=1,2,4,5)}$ the borehole wall was scanned from the top of the coal seam or the top surface of the caved zone 120 m upwards and transmitted to the computer for analysis. These measurements were conducted until the coal seam was extracted.

Finally, the macro-fractures in the walls of boreholes #1, #2, #4, and #5 induced by longwall mining were identified using the gray recognition technique (Tan *et al*. 2012). Various types of fractures were identified, such as fissures, dislocations, and splits. When examining the thickness of the fractured zones, fractures with an interval less than 1 m were considered as one macro-fracture. Fig. 8 shows the fractures in the borehole wall recorded 30-35 m above the top of the coal seam, for D_1 = 50 m. Fig. 9 shows dislocations on the wall of borehole #1, 50 m and 127 m above

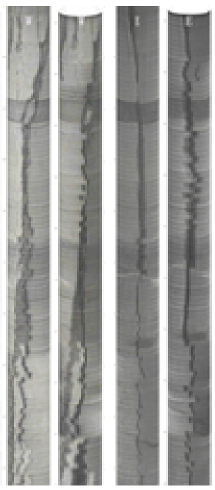

Fig. 8 Fractures on the wall of borehole #1, 30-35 m above the coal seam

(a) 50 m above the coal seam (b) 127 m above the coal seam

Fig. 9 Dislocation on the wall of borehole #1 the top of the coal seam. From these images, the fractures and dislocations in the overburden strata can be clearly identified.

4. Experimental results

4.1 Movement of overburden strata induced by close multiple-seam longwall mining

The displacement measured at borehole #3 with the advancement of Panel 20107 of coal seam No. 2-2^{upper} is shown in Fig. 10(a). H_i (i = 1, 2,..., 9, 10) was defined as the displacement of the rock strata at the position of anchor i. The displacement of the rock strata varied with the advancement of Panel 20107 (Fig. 10(a)). When $D_{3\text{-}1} = -5$ m, H_1 began to increase, indicating that the rock strata at the position of anchor #1 started to move. When $D_{3\text{-}1}$ = 2–10 m, H_1 quickly increased to 1000 mm and then the increment of H_1 diminished. When $D_{3\text{-}1}$ was about 200 m, H_1 reached a maximum of 1150 mm, which was approximately one quarter of the thickness of coal seam No. 2-2^{upper}. When $D_{3\text{-}1} = -2$ m, H_2 and H_3 begun to increase. At $D_{3\text{-}1}$ = 30–40 m, H_2 and H_3 similarly increased rapidly to 610 and 593 mm, respectively, then both displacements increased gradually with the advancement of Panel 20107. When $D_{3\text{-}1}$ was about 200 m, H_2 and H_3 reached a maximum of about 720 mm. This suggests that the strata monitored by anchors #2 and #3 moved as one rock unit when the longwall face was about 30–40 m from the borehole. Subsequently, H_4, H_5, and H_6 begun to increase in turn and then rapidly reached their maximum displacements, 478 mm, 380 mm, and 326 mm, corresponding to longwall advancing distances of $D_{3\text{-}1}$ = 60–70 m, 110 m, and 210 m, respectively. At $D_{3\text{-}1}$ = 280 m and 370 m, H_7, H_8, H_9, and H_{10} similarly increased, reaching maximum displacements of only 251, 232, 119, and 93 mm. These results indicate that the strata between anchors #7–#10 was not severely disturbed by the mining of Panel 20107 of coal seam No. 2-2^{upper}.

Combining the stratigraphic column data and the movement of the overburden strata, the following inferences can be obtained. As Panel 20107 of coal seam No. 2-2^{upper} advances, the strata movement can be divided into six rock groups with elevation above the top surface of the overlying strata 0–12.74 m, 12.74–46.59 m, 46.59–70.74 m, 70.74–89.54 m, 89.54–102.04 m, and 102.04–153 m above the coal seam. In addition, the longwall mining causes slight deformation at

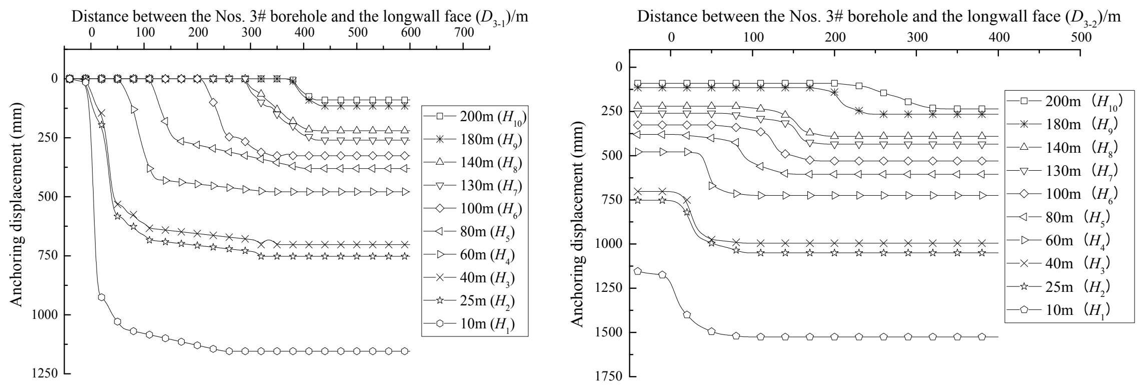

(a) After mining of Panel 20107 (b) After mining of Panel 20307

Fig. 10 Overburden displacements with advancing longwall face; H_i is the anchor location

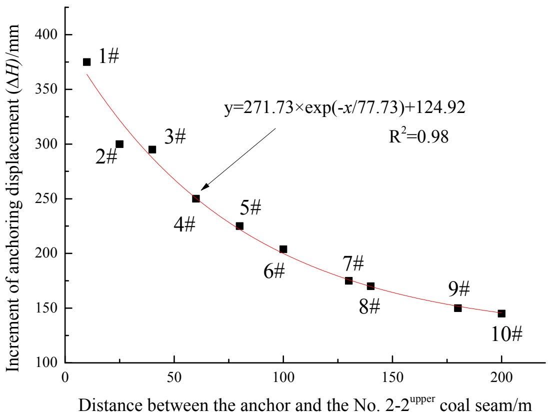

Fig. 11 Increment of anchor displacement after mining of Panel 20307 of coal seam No. 2-2^{middle}

the top of the overburden strata (elevation of 153 m above the upper seam surface).

The overburden displacement in borehole #3 with the advancement of Panel 20307 of coal seam No. 2-2^{middle} are shown in Fig. 10(b). When $D_{3\text{-}2}$ = 0–50 m, H_1, H_2, and H_3 increase almost at the same time. When $D_{3\text{-}2}$ = 100 m, H_1 reaches a maximum of 1150 mm while H_2 and H_3 were pproximately 1100 mm. The average rate of H_1 increase was 50 mm/day, which was larger than that of H_2 and H_3. The displacements H_1, H_2, and H_3 induced by the mining of coal seam No. 2-2^{middle} were 400, 300, and 295 mm, respectively. As shown in Figs. 10(a) and (b), the displacements H_4, H_5, H_6, and H_7(H_8) were about 250, 225, 203, and 175 mm, respectively, when Panel 20307 of seam No. 2-2^{middle} passed 400 m from borehole #3. The displacement of the overburden strata 102.04–180 m above the top surface of the coal seam increased slowly and the increment was only 150 mm.

Fig. 11 shows the displacement increment of the overburden during mining of the lower seam of No.2-2^{middle}. After Panel 20307 advances sufficiency, the overburden displacement increment has a negative exponent relation with the corresponding height above seam No. 2-2^{middle}. It can be approximated by the following formula

$$\Delta H = 271.73\exp(-x/77.73) + 124.92 \tag{1}$$

where ΔH is the displacement increment of the overburden strata, in mm; and x is the distance between the overburden strata and seam No. 2-2^{middle}, in m. A square regression coefficient of R^2 = 0.98 is obtained.

4.2 Overburden failures induced by close multiple-seam longwall mining

In our analysis, the caved zone was combined with the fractured zone into a single zone, which was named the failure zone. The thickness of the failure zone was the combined thickness of the caved zone and fractured zone (Fig. 7), which was defined as L_n (n = 1,2). When n = 1, L_1 is the height of the failure zone measured in boreholes #1 and #2. When n = 2, L_2 is the height of the failure zone measured in boreholes #4 and #5.

The height of the failure zone varied as the longwall face advanced (Fig. 12). The height of the failure zone gradually increased with the advancement of Panel 20107. When D_1 (D_2) ≤ 0, L_1 ≤ 2.5

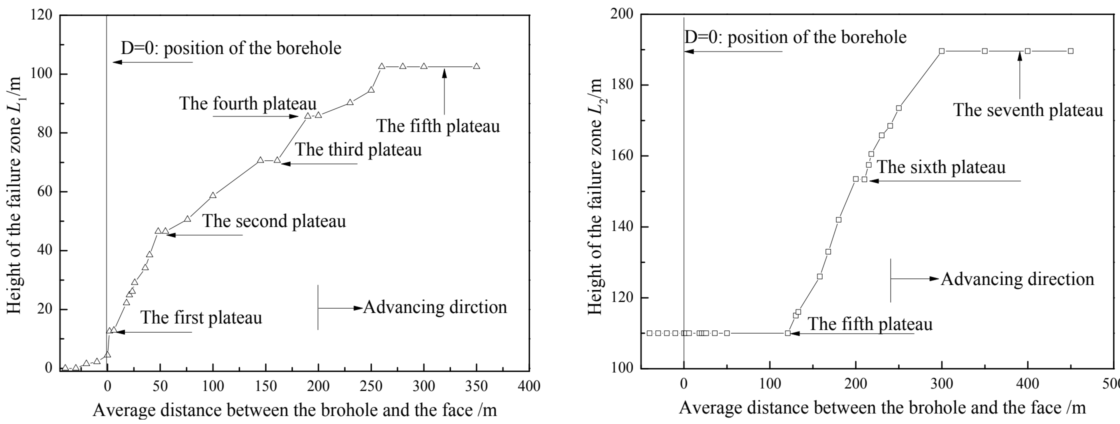

(a) After Panel 20107 advancing (b) After Panel 20307 advancing

Fig. 12 Height of the failure zone with the advancement of the longwall face

m, indicating that the rock layer failed 2.5 m above coal seam No. 2-2^{upper} when the working face of Panel 20107 did not pass the location of boreholes #1 and #2. For D_1 (D_2) = 2, L_1 = 12.9 m. For D_1 (D_2) = 2–8 m, the height of the failure zone remained constant. When D_1 (D_2) = 8–280 m, L_1 increased significantly from 12.9 m to 102.5 m and then remained constant as the longwall face of anel 20107 advanced. Thus, the maximum height of the failure zone was 102.5 m. In Fig. 12(a), five plateaus can be identified along the curves; the plateaus represent the stage where the height of the failure zone did not increase with the advancement of the longwall face. The heights of the five plateaus are L_1 = 12.9 m, 46.3 m, 70.8 m, 86.6 m, and 102.5 m, and the corresponding advancing distances D_1 (D_2) were 2–8 m, 35–40 m, 140–150 m, 185–198 m, and 210–350 m, respectively.

The height of the overburden failure zone measured in boreholes #4 and #5 with the advancement of the working face of Panel 20307 is shown in Fig. 12(b). When D_4 (D_5) = 0–130 m, L_2 = 102.5 m, indicating that the height of the failure zone did not vary when the working face was 130 m from boreholes #4 and #5. When D_4 (D_5) = 130–300 m, there are two plateaus along the curve where the height of failure zone did not increase with longwall face advancement. The height of the two plateaus are L_2 = 152.9 m and 189.6 m and the corresponding advancement D_4 (D_5) = 130–200 m, 200–300 m, respectively. These results suggest that the mining of Panel 20307 extended the failure zone upward to a height of 189.6 m.

5. Structures of the failure zone induced by close multiple-seam longwall mining

Previous studies found that when a longwall panel of sufficient width and length is excavated, the overburden strata are disturbed, with the most severe disturbance occurring near the immediate roof of the seam and decreasing toward the ground surface. Three distinct zones of overburden movement were identified: the caved zone, fractured zone, and continuous deformation zone. After coal extraction, the immediate roof fractures in an irregular pattern and falls directly into the caved zone. Above the caved zone is the fractured zone, where the main roof and the strata above it are broken into blocks. Between the fractured zone and the ground surface lays the continuous deformation zone. In this zone, the strata deform gently and behave essentially like a continuous or intact medium.

However, the main roof, which is composed of stratified, jointed and competent rock, may hang in the form of cantilever beams and fall into the caved zone after the face advances further (Yu *et al*. 2015). Field studies found that cantilever structures formed in the main roof in coal seams of the Ordos region coal fields. These findings may explain the plateaus on the failure zone height curves in relation to the position of the longwall face. The height of the failure zone increases ahead of the advancing face and then remains constant with further face advancement; however, once the hanging cantilever beam breaks and falls into the caved zone, the height of the failure zone begins to increase as the face continues to advance (Yu *et al*. 2015).

Based on the movement of the overburden strata and the position of the seven plateaus along the displacement curve, the rock overlying the mined coal seam can be divided into seven rock groups and three distinct zones (the caved zone, fractured zone, and continuous deformation zone); from this analysis we can derive the failure process of the overlying strata, in Fig. 13. When Panel 20107 of coal seam No. 2-2^{upper} advanced 2–10 m, the overlying strata 12.5 m above coal seam (the first rock group) shifted rapidly downward, suggesting that the first rock group caved into the gob and the height of the caved zone was 12.5 m. After Panel 20107 advanced 30–40 m, the overlying strata 12.74–46.59 m above the seam (the second rock group) deflected downward, and then collapsed into the caved zone. As discussed above, after Panel 20107 advanced 50–120 m, 110–200 m, and 210–280 m, respectively, the overlying strata 46.59–70.74 m, 70.74–89.54 m, and 89.54–102.04 m above the coal seam formed the third to the fifth rock group. The second to fifth rock group constituted the fractured zone, with a thickness of 102.04 m. Analysis of the stratigraphic columns and strata behavior patterns shows that each rock group in the fractured zone generally consists of sub-layers. Each sub-layer appears to comprise an upper thin layer and a lower thick layer of rock. Here we use the second rock group as an example to illustrate the group characteristics. The layer in the lower portion of the second rock group is mudstone with a thickness of 20.95 m; the middle portion is a 6.78-m-thick layer of sandy mudstone. The upper portion is a layer of 6.12-m-thick mudstone. The strata above the fifth rock group show gentle deformation. No cracks were detected by the DPID along the borehole, which indicates that the

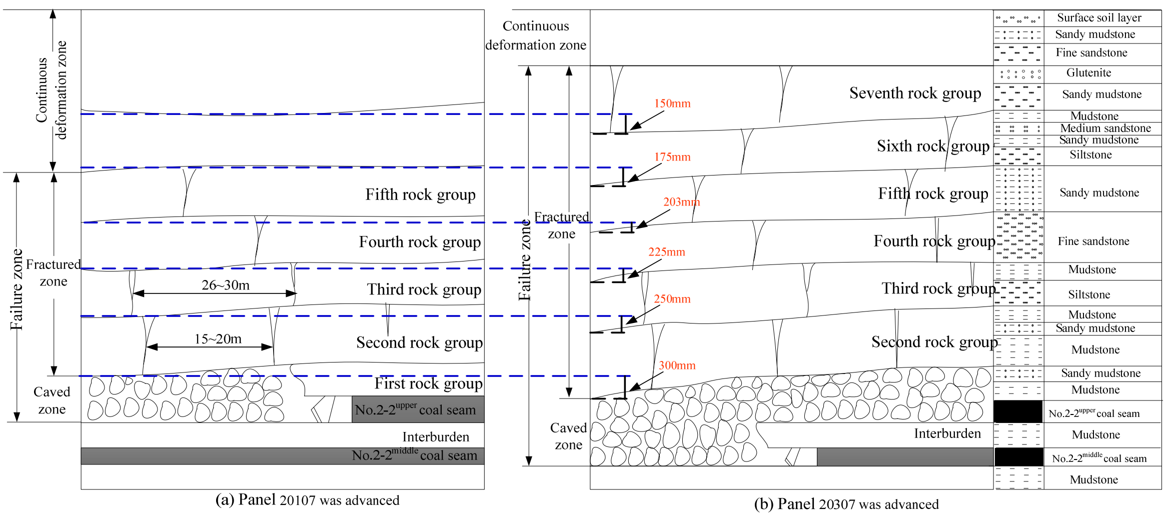

Fig. 13 Structure of overburden above close multiple-seam longwall mining

overlying strata in this range formed a continuous deformation zone.

When Panel 20307 of coal seam No. 2-2$^{\text{middle}}$ advanced 5–10 m, the interburden between the upper and lower seams caved and then the caving zones of the upper and lower seams merged. Downward sagging of the strata occurred at the lowest stratum of the fractured zone and ropagated upward. Then, a gap (400 mm wide) developed between the fractured zone and the continuous deformation zone. As shown in Figs. 10(b) and 12(b), the sixth and seventh rock groups (strata 102.5–152.9 m and 152.9–189.6 m above seam No. 2-2$^{\text{upper}}$), previously located in the continuous deformation zone, sag downward, and then fall into the fractured zone after the longwall face of Panel 20307 advances 130–200 m and 200–300 m from boreholes #4 and #5, respectively. The thicknesses of the sixth and seventh failure zones were 50.4 m and 36.7 m, respectively, adding up to a total failure zone thickness of 87.1 m.

Previous studies found that the support in the face area was greatly affected when a hanging cantilever beam in the lower portion of the fractured zone broke and fell into the caved zone. The broken length of the cantilever beam is known as a periodic roof weighting interval. Generally, the periodic roof weighting interval varies with the condition of the rock layer. To determine the periodic roof weighting interval, we laid pressure cells to support the longwall face of Panel 20107 and measured the support resistance in the field. Then, the method of support resistance monitoring (Yu *et al*. 2015) was used to determine the periodic roof weighting interval. In this longwall face, the periodic roof weighting interval of the second rock group ranged from 15 to 20 m and that of the third rock group was 26–30 m.

6. New statistical formula for predicting the height of the failure zone above multi-seam coal mining

The height of the failure zone above the multi-seam coal mining area varies with the buried depth of the coal seam, rock layers, and interburden thickness. An empirical criterion predicting the height of the failure zone (National Coal Ministry Administration of China 2000) was developed in China based on data from various multi-seam coal mining scenarios.

$$M = M_2 + \left[M_1 - h_{1-2}(K_A - 1)\right] \tag{2}$$

$$H_{\max} = \frac{100\sum M}{1.6\sum M + 2.2} \pm 5.6 \tag{3}$$

where M is the overall mining height when the upper and lower coal seams were both mined, in m; $H_{\max}$ is the maximum height of the failure zone, in m; M_1 and M_2 are the mining heights of the upper and lower coal seams, respectively, in m; $h_{1\text{-}2}$ is the thickness of the interburden, in *m*; and K_A is the bulking factor. Commonly, the used value for the bulking factor range from 1.2 to 1.25.

In the Gaojialiang mine, M_1 = 4.1 m, M_2 = 5.2 m, $h_{1\text{-}2}$ = 9.5 m, and K_A = 1.2. Using Eq. (2) we obtain M = 7.4 m. According to Eq. (3), the maximum height of the failure zone $H_{\max}$ = 47.11–58.31 m. However, field measurements in the mine show that the maximum height of the failure zone was 189.6 m after Panel 20307 of seam No. 2-2$^{\text{middle}}$ advanced sufficiently. This value is much higher than the ones obtained from the Eqs. (2) and (3), indicating that Eqs. (2) and (3) cannot be used to predict the height of the failure zone for close multiple-seam longwall mining in the Ordos region, especially when the coal seams are overlain by a very thick layer of soft rock

Table 1 The maximum height of failure zone with soft rock onerburden with close multiple-seam longwall mining

Experimental site	Longwall face	h_{1-2}(m)	H (m)	M (m)	H_{max} (m)	Experimental method	Ref.
Gaojialiang mine	20107 and 20307	9.5	210.3~230.5	7.4	189.6	DMPX and DPID	This study
Halagou mine	20207 and 20206	12.5	160.3~180.4	5.2	120.65	Borehole discharge	Peng *et al.* 2015
Jinyang mine	20307 and 20307	14.6	165.3~192.6	4.1	77.431	Borehole discharge	Peng *et al.* 2015
Yujialiang mine	20407and 20406	18.8	165.3~192.6	3.5	72.865	Borehole discharge	Peng *et al.* 2015
Luxin mine	2103 and 2204	7.5	258.1~271.2	8.6	240.5	Numerical simulation	Tian *et al.* 2014
Luxin mine	2105 and 2206	6.5	352~372.6	8.0	210.5	Borehole discharge	Zhang 2012
Bulianta mine	31404 and 31505	13.5	178.2~195.3	6.5	156.3	Borehole discharge	Peng *et al.* 2015
Bulianta mine	31404 and 31505	11.2	187.2~197.5	5.9	136.2	Borehole discharge	Peng *et al.* 2015

*Note: H was the mining depth; h_{1-2} is thickness of the interburden between the upper coal seam and lower coal seam; M is the comprehensive mining height when the upper and lower coal seams were both mined, which can be obtained using the Eq.(2); H_{max} is the maximum height of the failure zone

with poor cementation.

In the following, the datasets from this investigation and Ref (Zhang 2012, Tian *et al.* 2014, Peng *et al.* 2015) were utilized to derive a formula for the maximum height of the failure zone. Table 1 lists the physical parameters of the failure zones and the coal seams that were used to ollect data of close multiple-seam longwall mining in the Ordos region. These data were obtained by numerical simulation and field investigations in cases where the overburden strata of the longwall mined seams were comprised of very thick soft rock with poor cementation. The relationship between the height of the failure zone and the overall mining height is shown in Fig. 14. Using a linear regression function, the maximum height of the failure zone can be approximated by the following formula

$$H_{\max} = 29.08M - 33.39 \tag{4}$$

where H_{max} and M are in units of m. This yields a square regression coefficient of R_2 = 0.98844. This formula is suitable for $3.5 \leq M \leq 8.6$ m. The interburden caved into the gob behind the support after the lower coal seam was mined.

Eq. (4) shows that the height of the failure zone H_{max} increases linearly with overall mining height M. Comparing the height calculated by Eq. (4) with the data listed in Table 1, the maximum absolute error of H_{max} is 8.41 m. For Panels 20107 and 20307 in the Gaojialiang mine, after the

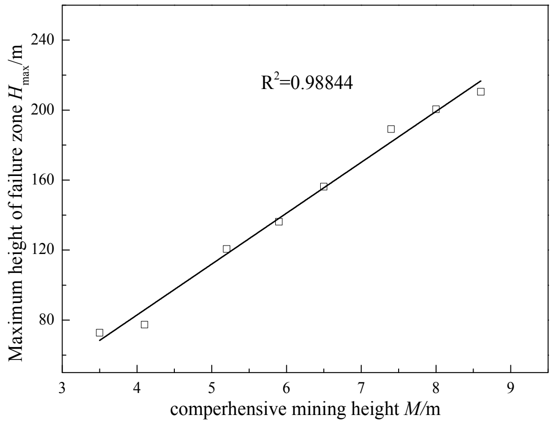

Fig. 14 Comparison of observed and calculated values of the maximum height of the failure zone

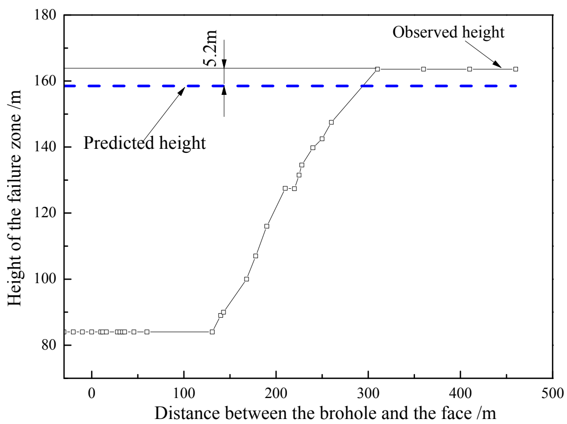

Fig. 15 Comparison of observed and calculated values of the maximum height of the failure zone

upper and lower coal seams were mined, the overall mining height was M = 7.4 m and the height of the failure zone H_{max} was 181.8 m using Eq. (4) with a maximum absolute error of 7.8 m. In the field survey the maximum height of the failure zone was 189.6 m.

Panels 20106 and 20306 in the Gaojialiang mine are adjacent to Panels 20107 and 20307, and are used to extract from coal seams No. 2-2^{upper} and No. 2-2^{middle}, respectively. The geological and mining conditions of Panels 20106 and 20306 are similar to those of Panels 20107 and 20307. In previous studies, DPID was used to determine the longwall mining-induced strata failure of Panels 20106 and 20306, and the maximum height of the failure zone was 163.7 m. Using Eq. (4), the overall mining height was 6.6 m and H_{max} was 158.5 m. The maximum absolute error is 5.2 m (Fig. 15), which is in the range of the errors obtained for this formula.

7. Conclusions

In China, close multiple-seam longwall mining has been successfully practiced in the Ordos coalfield. To understand the mining-induced strata behavior in close multiple-seam longwall mining, in-situ investigations were conducted in Panel 20107 of coal seam No. 2-2^{upper} and Panel 20307 of coal seam No. 2-2^{middle} of the Gaojialiang mine. The results of the investigations presented in this paper can be summarized as follows.

- By using the DMPX and DPID, the strata displacement and clear images of cracks and dislocations were obtained as the upper and lower coal seams were mined. Based on the measured data, three distinct zones (the caved zone, fractured zone, and continuous deformation zone) were identified in the strata overlying the multiple-seam longwall mining. The strata overlying seam No. 2-2^{upper} was 102.04 m high and formed a continuous deformation zone.
- Based on the relation between the failure heights and the advancement of the longwall faces, a clear structure of the overburden failure zones was obtained and seven rock groups were identified. After the longwall face of Panel 20107 of seam No. 2-2^{upper} advanced, the overburden strata were damaged, with the most severe deformation occurring near the immediate roof of the seam and decreasing toward the surface. The caved zone extends 12.9 m above the top surface of the coal seam (first rock group). The second to fifth rock groups form the fractured zone, with a maximum failure zone height of 102.04 m. Then, after Panel 20307 of coal seam No. 2-2^{middle} advanced, a 400-mm gap formed between the fractured zone and the continuous deformation zone. The lowest stratum in the continuous deformation zone, consisting of the sixth and seventh rock groups, fell into the fractured zone, and the failure zone increased 87.1m in thickness.
- With further processing of the data of the failure zone obtained in our in-situ investigations and other relevant sources, a statistical formula ($H_{f\max} = 29.08M - 33.39$) is presented to estimate the maximum height of the failure zone for a very thick, soft overlying strata with poor cementation above close multiple-seam longwall mining.

Acknowledgments

This study was supported by National Natural Science Foundation of China (No. 51574154, 51274133, 51474137), Shandong province science and technology development plan item (2014GSF120002), Tai'shan Scholar Engineering Construction Fund of Shandong Province of China, and Postgraduate Innovative Fund Project of Shandong University of Science and Technology (YC150308).

References

Gao, F.Q., Stead, D. and Coggan, J. (2014), "Evaluation of coal longwall caving characteristics using an innovative UDEC Trigon approach", *Comput. Geotech.*, **55**, 448-460.

Guo, H., Yuan, L. and Shen, B.T. (2012), "Mining-induced strata stress changes, fractures and gas flow dynamics in multi-seam longwall mining", *Int. J. Rock Mech. Min. Sci.*, **54**, 129-139.

Jin, X.L, and Zhang, H. (2010), "Distributing Features of Jurassic Coal Measures Hydrocarbon Source Rock in Northeastern Ordos Basin", *J. Coal Geol. China*, **22**(1), 15-19.

Karacan, C.Ö. and Olea, R.A. (2014), "Inference of strata separation and gas emission paths in longwall overburden using continuous wavelet transform of well logs and geostatistical simulation", *J. Appl. Geophys.*, **105**, 147-158.

Khanal, M., Adhikary, D. and Jayasundara, C. (2016), "Numerical study of mine site specific multiseam mining and its impact on surface subsidence and chain pillar stress", *Geotech. Geol. Eng.*, **34**(1), 217-235.

Liu, X.S, Tan, Y.L. and Ning, J.G. (2015), "The height of water-conducting fractured zones in longwall mining of shallow coal seams", *Geotech. Geol. Eng.*, **33**(3), 693-700.
Ma, L.Q., Du, X. and Wang, F. (2013), "Water-preserved mining technology for shallow buried coal seam in ecologically-vulnerable coal field: A case study in the Shendong coal field of China", *Disaster Adv.*, **6**, 268-278.
Miao, X.X., Cui, X.M. and Wang, J.A. (2011), "The height of fractured water-conducting zone in undermined rock strata", *Eng. Geol.*, **120**(1), 32-39.
Peng, S.S., Li, H.M. and Zhou, Y. (2015), *Ground Control in the Ordos Coal Field*, China Science Press, Beijing, China.
Palchik, V. (2010), "Experimental investigation of apertures of mining-induced horizontal fractures", *Int. J. Rock Mech. Min. Sci.*, **47**(3), 502-508.
Rezaei, M., Hossaini, M.F. and Majdi, A. (2015), "Determination of longwall mining-induced stress using the strain energy method", *Rock Mech. Rock Eng.*, **48**(6), 2421-2433.
Sui, W.H., Hang, Y. and Ma, L.X. (2015), "Interactions of overburden failure zones due to multiple-seam mining using longwall caving", *Bull. Eng. Geol. Environ.*, **74**(3), 1019-1035.
Tan, Y.L., Ning, J.G. and Li, H.T. (2012), "In situ explorations on zonal disintegration of roof strata in deep coalmines", *Int. J. Rock Mech. Min. Sci.*, **49**, 113-124.
Tian, C.L., Ning, J.G. and Tan, Y.L. (2014), "Shallow Overburden rock fracture zone development law under many mining conditions", *Safe. Coal Min.*, **45**(11), 45-47.
Tan, Y.L., Liu, X.S., Ning, J.G. and Lu, Y.W. (2017), "In situ investigations on failure evolution of overlying strata induced by mining multiple coal seams", *Geotech. Test. J.*, **40**(2), 244-257.
Tulu, I.B., Esterhuizen, G.S. and Klemetti, T. (2016), "A case study of multi-seam coal mine entry stability analysis with strength reduction method", *Int. J. Min. Sci. Technol.*, **26**(2), 193-198.
Wang, F.T., Zhang, C. and Zhang, X.G. (2015), "Overlying strata movement rules and safety mining technology for the shallow depth seam proximity beneath a room mining goaf", *Int. J. Min. Sci. Technol.*, **25**(1), 139-143.
Wang, F.T., Tu S.H. and Zhang, C. (2016), "Evolution mechanism of water-flowing zones and control technology for longwall mining in shallow coal seams beneath gully topography", *Environ. Earth Sci.*, **75**(19), 1309.
Xiong, Z.Q., Wang C. and Zhang, N.C. (2015), "A field investigation for overlying strata behaviour study during protective seam longwall overmining", *Arab. J. Geosci.*, **8**(10), 7797-7809.
Yu, B., Zhao, J. and Kuang, T.J. (2015), "In situ investigations into overburden failures of a super-thick coal seam for longwall top coal caving", *Int. J. Rock Mech. Min. Sci.*, **4**(78), 155-162.
Zhang, M. (2012), "Research on mining-induced overburden failures and its application in aquifer protection during longwall mining of shallow coal seams with a mass soft rock", Ph.D. Dissertation; Shandong University of Science and Technology, Qingdao, China.
Zhang, D.S., Fan, G.W. and Ma, L.Q. (2011), "Aquifer protection during longwall mining of shallow coal seams: a case study in the Shendong Coalfield of China", *Int. J. Coal Geol.*, **86**(2), 190-196.
Zhang, J.G., Miao X.X. and Huang, Y.L. (2014), "Fracture mechanics model of fully mechanized top coal caving of shallow coal seams and its application", *Int. J. Min. Sci. Technol.*, **24**(3), 349-352.
Zhao, C.B. (2015), "Analytical solutions for crack initiation on floor-strata interface during mining", *Geomech. Eng., Int. J.*, **8**(2), 237-255.

CC